Journal of Thermal Analysis, Vol. 48 (1997) 877-884

SYNTHESIS AND DEHYDRATION OF DOUBLE OXALATES OF RARE EARTHS(III) WITH SOME MONOVALENT METALS

II. Investigations of $RbLn(C_2O_4)_2 \cdot nH_2O$

O. Genčova[1] *and J. Šiftar*[2]

[1]Institute of Chemistry, Faculty of Science, 'St. Cyril and Methodius' University, 91000 Skopje, Macedonia
[2]Department of Chemistry and Chemical Technology, University of Ljubljana, Ljubljana, Slovenia

(Received July 20, 1995; in revised form February 10, 1996)

Abstract

Double oxalates of rare earths(III) and rubidium with the general formulae $RbCe(C_2O_4)_2 \cdot 4.5H_2O$, $RbLn(C_2O_4)_2 \cdot 4H_2O$ (*Ln*=Yb, Lu), $RbLn(C_2O_4)_2 \cdot 3.5H_2O$ (*Ln*=La, Pr–Dy), and $RbLn(C_2O_4)_2 \cdot 3H_2O$ (*Ln*=Ho, Er, Tm, Y) were synthesized. They were characterized by chemical analysis, TG, DTG and DSC over the temperature interval 20–500°C and X-ray powder diffraction examination. At the chosen final temperature (500°C), either oxide (Ln_2O_3) or basic carbonate $Ln_2O_2CO_3$) and Rb_2CO_3 were obtained, depending on the rare earth(III) element. On the basis of the X-ray diffraction patterns, the isolated compounds can be divided into five isostructural groups.

Keywords: double oxalates, rare earths (lanthanons), rubidium

Introduction

As a continuation of work on the synthesis and characterization of double oxalates of trivalent and monovalent cations [1, 2], this paper reports on the oxalatometallates of rare earths(III) and rubidium. A survey of the literature did not reveal any substantial data on oxalatometallates of rare earths and rubidium.

The synthesis and thermal characterization of $RbEu(C_2O_4)_2 \cdot 3H_2O$ [3] and $RbGd(C_2O_4)_2 \cdot nH_2O$ [4] were recently described.

In the present study, we investigated the thermal behaviour of all the isolated compounds and determined the isostructural groups.

Experimental

Reagents and methods

The procedure for the synthesis of double oxalates of the rare earths(III) and monovalent cations is given in Part 1 of this study [5].

0368–4466/97/ $ 5.00

John Wiley & Sons, Limited
Chichester

Table 1 Analytical data of the compounds and calculated values

	Compound	Found/%			Calculated/%			
		Ln	C_2O_4	H_2O	Ln	C_2O_4	H_2O	Rb
1	$RbLa(C_2O_4)_2 \cdot 3.5H_2O$	29.60	38.06	13.10	29.97	37.98	13.60	18.44
2	$RbCe(C_2O_4)_2 \cdot 4.5H_2O$	30.07	36.02	16.62	29.03	36.49	16.78	17.71
3	$RbPr(C_2O_4)_2 \cdot 3.5H_2O$	30.92	36.80	12.65	30.28	37.82	13.54	18.36
4	$RbNd(C_2O_4)_2 \cdot 3.5H_2O$	30.01	37.49	13.37	30.77	37.55	13.45	18.23
5	$RbSm(C_2O_4)_2 \cdot 3.5H_2O$	31.78	37.26	12.46	31.66	37.07	13.28	17.99
6	$RbGd(C_2O_4)_2 \cdot 3.5H_2O$	32.30	36.59	12.45	32.65	36.54	13.08	17.74
7	$RbTb(C_2O_4)_2 \cdot 3.5H_2O$	32.50	35.65	13.22	32.88	36.41	13.03	17.68
8	$RbDy(C_2O_4)_2 \cdot 3.5H_2O$	32.94	35.98	13.27	33.36	36.14	12.95	17.55
9	$RbHo(C_2O_4)_2 \cdot 3.0H_2O$	34.43	36.30	11.31	34.33	36.64	11.25	17.79
10	$RbEr(C_2O_4)_2 \cdot 3.0H_2O$	34.00	36.84	11.32	34.65	36.46	11.19	17.70
11	$RbTm(C_2O_4)_2 \cdot 3.0H_2O$	34.81	36.16	11.06	34.87	36.34	11.16	17.64
12	$RbYb(C_2O_4)_2 \cdot 4.0H_2O$	33.89	34.73	14.25	34.16	34.75	14.22	16.87
13	$RbLu(C_2O_4)_2 \cdot 4.0H_2O$	34.44	33.98	13.98	34.41	34.62	14.17	16.81
14	$RbY(C_2O_4)_2 \cdot 3.0H_2O$	21.61	42.58	13.69	21.98	43.52	13.36	21.13

The thermogravimetric (TG), derivative thermogravimetric (DTG) and DSC curves were obtained on a Thermal Analyst 2000 (E.I. DuPont, Wilmington DE) in a flow of dry air. The same thermoanalytical methods and experimental conditions were used as for the examination of the double oxalates of the rare earths(III) with the general empirical formula $RbLn(C_2O_4)_2{\cdot}nH_2O$ described in [5].

Powder photographs with a Guinier de Wolf camera with CuK_α radiation were taken for all isolated compounds. The Guinier diagrams were not very sharp. The X-ray powder diffraction patterns are not presented.

Results and discussion

Analytical results are given in Table 1, together with the calculated values. The percentage of H_2O was obtained by thermogravimetric measurements.

The compounds in Table 1 were isolated from a starting mixture with a molar ratio $Rb_2C_2O_4$: $Ln^{3+}=5:1$, at a *pH* around 6. The tabulated data reveal the stoichiometry $RbLn(C_2O_4)_2{\cdot}nH_2O$ ($n=3.5$ for Ln=La, Pr–Dy; $n=3.0$ for Ln=Ho, Er, Tm, Y; $n=4.0$ for Yb, Lu; and $n=4.5$ for Ce).

On the basis of the X-ray diffraction patterns, the isolated compounds can be divided into the following five isostructural groups:

1. $RbLn(C_2O_4)_2{\cdot}3.5H_2O$ (Ln=La)
2. $RbLn(C_2O_4)_2{\cdot}4.5H_2O$ (Ln=Ce)
3. $RbLn(C_2O_4)_2{\cdot}3.5H_2O$ (Ln=Pr, Nd, Sm, Gd, Tb, Dy)
4. $RbLn(C_2O_4)_2{\cdot}3.0H_2O$ (Ln=Ho, Er, Tm, Y)
5. $RbLn(C_2O_4)_2{\cdot}4.0H_2O$ (Ln=Yb, Lu)

For more details, single-crystal structures of representatives of all five groups will be needed. TG, DTG and DSC curves of the obtained compounds are given in Figs 1(a)–(h) and Figs 2(a)–(h). The thermal decomposition of the compounds takes place in two stages. The first step is thermal dehydration, and the second is the exothermic oxidation of oxalate ion.

The complexes $RbLa(C_2O_4)_2{\cdot}3.5H_2O$ and $RbCe(C_2O_4)_2{\cdot}4.5H_2O$ lose all their water in a single stage, with an endothermic peak at 151.79°C (La) or 126.06°C (Ce). For the elements from Pr to Y, the course of dehydration proceeds through several steps. The first and second steps for the compounds from Sm to Er and Pr and Yb correspond to the formation of the intermediate 0.75 hydrate, while the final step of dehydration for the Nd compound corresponds to the formation of the 1.25 hydrate, for that of Tm to the 0.5 hydrate, for that of Lu to the 1.5 hydrate and for that of Y to the monohydrate. The Pr to Y compounds appear to contain additional zeolitic water which is lost at low temperature. Similar studies have been performed on the complexes $K_3[Ln(Ox)_3(OH_2)]{\cdot}2H_2O$ [6].

The last step for all compounds gave the dehydrated salt. The decomposition of the anhydrous double oxalates in the temperature range from 300 to 550°C takes place in four stages:

1. $Ln_2(C_2O_4)_3 \rightarrow Ln_2O_2CO_3 + 3CO + 2CO_2$
2. $2CO + O_2 \rightarrow 2CO_2$

3. $Rb_2C_2O_4 \rightarrow Rb_2CO_3 + CO$
4. $Ln_2O_2CO_3 \rightarrow Ln_2O_3 + CO_2$

A survey of the DSC curves demonstrates that the first three reactions are exothermic. It is difficult to explain the role of the oxidation of carbon monoxide. Work in an inert atmosphere does not give an answer, because in this case elemental carbon is obtained. At the chosen final temperature (only 500°C), either rare earth oxide or basic carbonate and Rb_2CO_3 were obtained, depending on the rare earth

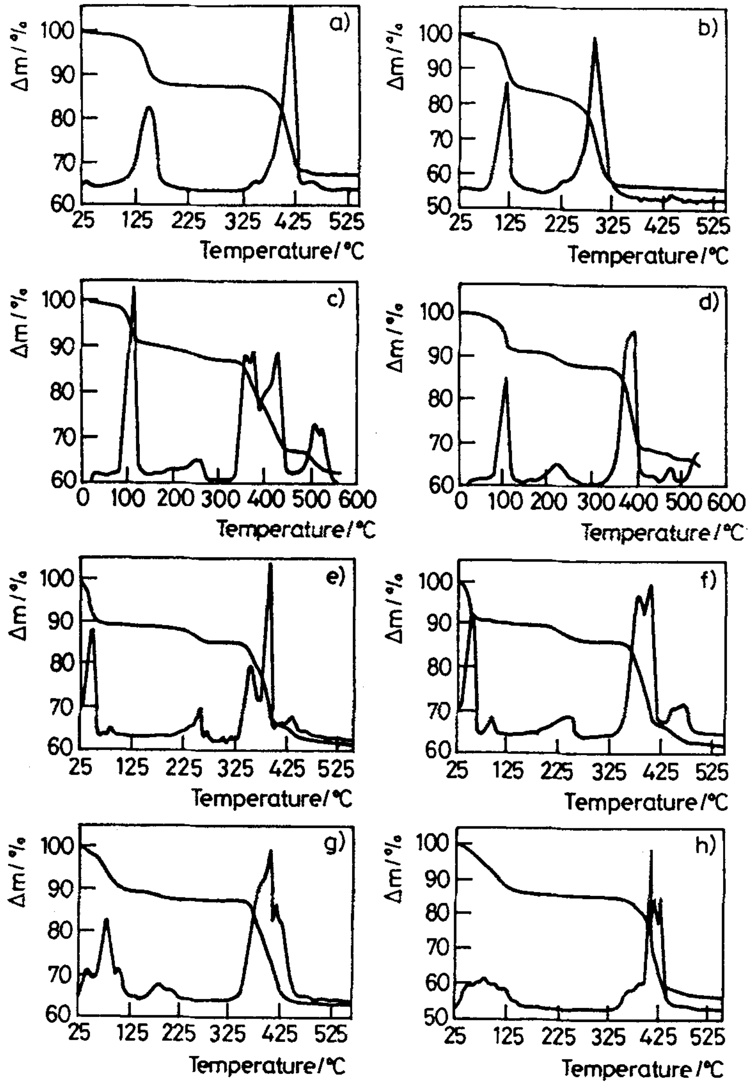

Fig. 1 TG and DTG curves of $RbLn(C_2O_4)_2 \cdot nH_2O$ (where Ln is La (a), Ce (b), Pr (c), Sm (d), Tb (e), Dy (f) and Tm (g) and n is 3.0 (g), 3.5 (a, c, d, e, f), 4.0 (h) and 4.5 (b)

element. An exception was the decomposition of the cerium complex, where this maximum was reached at 378.4°C, probably because of the formation of CeO2. Oxicarbonate intermediates are well known in the thermal decomposition of lanthanide oxalates [7, 8]. The presence of carbonate was confirmed via its characteristic reaction with acids. The final product of thermal decomposition was identified from the X-ray powder diffraction pattern of the residue, and from the theoretical values and experimental results (Table 2). Exothermic peaks in the DSC curves for

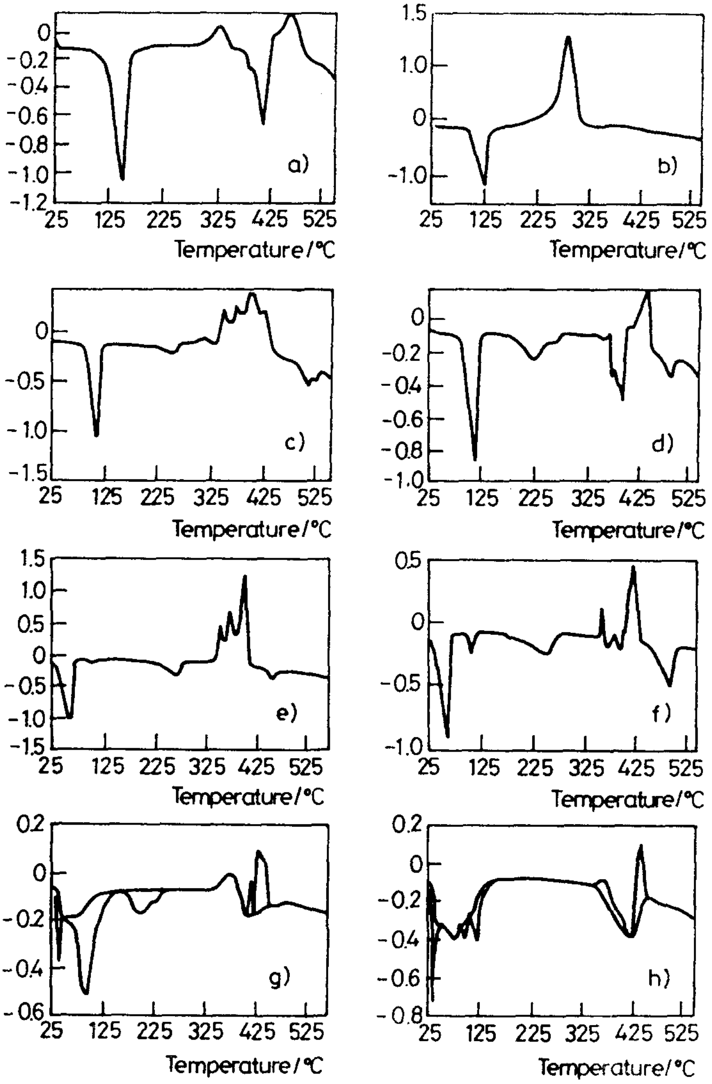

Fig. 2 DSC curves of $RbLn(C_2O_4)_2{\cdot}nH_2O$ (where Ln is La (a), Ce (b), Pr (c), Sm (d), Tb (e), Dy (f) and Tm (g) and n is 3.0 (g), 3.5 (a, b, c, d, e, f) and 4.0 (h)

Table 2 TG analysis of $RbLn(C_2O_4)_2{\cdot}nH_2O$

	Compound	*T*/K		Effect fragment	$\Delta m_{exp.}$/ %	$\Delta m_{calc.}$/ %
		starting	final			
1	$RbLa(C_2O_4)_2{\cdot}3.5H_2O$	607.35	763.85	$La_2O_3{\cdot}2CO_2$ $+Rb_2CO_3$	32.92	31.81
2	$RbCe(C_2O_4)_2{\cdot}4.5H_2O$	459.65	651.55	$2CeO_2$ $+Rb_2CO_3$	42.95	40.41
3	$RbPr(C_2O_4)_2{\cdot}3.5H_2O$	557.95	810.75	$Pr_2O_3{\cdot}CO_2$ $+Rb_2CO_3$	37.03	38.56
4	$RbNd(C_2O_4)_2{\cdot}3.5H_2O$	590.65	787.75	$Nd_2O_3{\cdot}CO_2$ $+Rb_2CO_3$	34.66	34.77
5	$RbSm(C_2O_4)_2{\cdot}3.5H_2O$	575.95	773.05	$Sm_2O_3{\cdot}CO_2$ $+Rb_2CO_3$	33.60	34.32
6	$RbGd(C_2O_4)_2{\cdot}3.5H_2O$	604.85	816.85	Gd_2O_3 $+Rb_2CO_3$	37.16	38.40
7	$RbTb(C_2O_4)_2{\cdot}3.5H_2O$	579.55	754.95	Tb_2O_3 $+Rb_2CO_3$	35.86	38.27
8	$RbDy(C_2O_4)_2{\cdot}3.5H_2O$	592.25	762.55	Dy_2O_3 $+Rb_2CO_3$	37.12	37.99
9	$RbHo(C_2O_4)_2{\cdot}3.0H_2O$	597.25	743.65	Ho_2O_3 $+Rb_2CO_3$	35.07	36.64
10	$RbEr(C_2O_4)_2{\cdot}3.0H_2O$	604.85	768.85	Er_2O_3 $+Rb_2CO_3$	35.40	36.46
11	$RbTm(C_2O_4)_2{\cdot}3.0H_2O$	602.25	751.25	Tm_2O_3 $+Rb_2CO_3$	36.58	36.33
12	$RbYb(C_2O_4)_2{\cdot}4.0H_2O$	603.55	752.45	Yb_2O_3 $+Rb_2CO_3$	41.93	38.30
13	$RbLu(C_2O_4)_2{\cdot}4.0H_2O$	603.55	753.75	Lu_2O_3 $+Rb_2CO_3$	37.55	38.15
14	$RbY(C_2O_4)_2{\cdot}3.0H_2O$	603.55	767.65	Y_2O_3 $+Rb_2CO_3$	42.65	43.52

Table 3 The dehydration enthalphy function ΔH calculated from DSC-curves in kJ mol^{-1} H_2O

	Compound	ΔH_{calc} for different stages of dehydration/kJ mol^{-1} H_2O				ΔH_{calc} for total dehydration/kJ mol^{-1} H_2O
		I	II	III		
1	$RbLa(C_2O_4)_2 \cdot 3.5H_2O$	51	–	–		51
2	$RbCe(C_2O_4)_2 \cdot 4.5H_2O$	36	–	–		36
3	$RbPr(C_2O_4)_2 \cdot 3.5H_2O$	43	16	–		36
4	$RbNd(C_2O_4)_2 \cdot 3.5H_2O$	51	19	–		38
5	$RbSm(C_2O_4)_2 \cdot 3.5H_2O$	42	36	–		40
6	$RbGd(C_2O_4)_2 \cdot 3.5H_2O$	48	50	44		47
7	$RbTb(C_2O_4)_2 \cdot 3.5H_2O$	50	68	–		55
8	$RbDy(C_2O_4)_2 \cdot 3.5H_2O$	49	44	67		53
9	$RbHo(C_2O_4)_2 \cdot 3.0H_2O$	41	54	–		45
10	$RbEr(C_2O_4)_2 \cdot 3.0H_2O$	10	53	54		49
11	$RbTm(C_2O_4)_2 \cdot 3.0H_2O$	18	44	69	13.98	39
12	$RbYb(C_2O_4)_2 \cdot 4.0H_2O$	–	–	–		14
13	$RbLu(C_2O_4)_2 \cdot 4.0H_2O$	27	11	5		12
14	$RbY(C_2O_4)_2 \cdot 3.0H_2O$	46	57	–		49

Rb and in the DTA curves for K [5] were probably due to crystal modifications (phase transitions) of Ln2O3, and also to the work in the Pt crucibles in an air atmosphere, because Pt catalyses the conversion of CO to CO2, which is a highly exothermic reaction.

We have also investigated the trends in the magnitude of the dehydration enthalpy function, ΔH. All the values are calculated in kJ mol^{-1} H_2O. The corresponding heats of reactions from the DSC curves fall in the range 12–55 kJ mol^{-1} H_2O. The ΔH values are shown in Table 3, where a good correlation was not obtained. It can be seen from the DSC curve for the complex of Yb that the dehydration process occurs in a stepwise way. The three stages of water loss are observed in the DSC curve (Fig. 2(h)), but there is not a distinct separation of the dehydration stages in the TG curve (Fig. 1(h)), and hence we give the total value of the enthalpy (14 kJ mol^{-1} H_2O).

References

1 N. Bulc, J and Šiftar, Acta Crystallogr., C39, (1983) 176.
2 O. Genčova and J. Šiftar, J. Thermal Anal., 44, (1995) 1171.
3 M. E. Modebadze, N. G. Sheliya and L. N. Kargareteli, Issled. Obl. Khim. Kompleksn. Prostykh Soed. Nekot. Perekh. Red. Met., 3 (1978) 121, Chem. Abstr. 90 (1979) 214499b.
4 E. G. Davitashvili, M. E. Modebadze and N. G. Sheliya, Soobskh. AN GRUZ SSR, 73 (1974) 65, Chem. Abstr., 80 (1974) 103355a.

5 O. Genčova and J. Šiftar, J. Thermal Anal., 48, (1997) 321.
6 I. A. Kahwa, F. R. Fronczek and J. Selbin, Inorg. Chim. Acta, 82 (1984) 161.
7 R. Möbius and F. Matthes, J. Inorg. Nucl. Chem., 28 (1966) 1601.
8 A. Glasner and M. Steinberg, J. Inorg. Nucl. Chem., 22 (1961) 39.